AWARD NUMBER: W81XWH-19-1-0378

TITLE: Combining Androgen Deprivation and Immunotherapy to Prevent Progression to Castration-Resistant Prostate Cancer

PRINCIPAL INVESTIGATOR: Kent L. Nastiuk, Ph.D

CONTRACTING ORGANIZATION: Health Research, Inc.
Health Research-Roswell Park Cancer
Elm and Carlton St.
Buffalo, New York 14263-0001

REPORT DATE: OCTOBER 2023

TYPE OF REPORT: Annual

PREPARED FOR: U.S. Army Medical Research and Development Command
Fort Detrick, Maryland 21702-5012

REPORT DOCUMENTATION PAGE

Form Approved
OMB No. 0704-0188

1. REPORT DATE	2. REPORT TYPE	3. DATES COVERED
OCTOBER 2023	Annual	1 Sept 2022-31 Aug 2023

4. TITLE AND SUBTITLE

Combining Androgen Deprivation and Immunotherapy to Prevent Progression to Castration-Resistant Prostate Cancer

5a. CONTRACT NUMBER
W81XWH-19-1-0378

5b. GRANT NUMBER

5c. PROGRAM ELEMENT NUMBER

6. AUTHOR(S)
Kent L. Nastiuk, PhD

E-Mail: kent.nastiuk@roswellpark.org

5d. PROJECT NUMBER

5e. TASK NUMBER

5f. WORK UNIT NUMBER

7. PERFORMING ORGANIZATION NAME(S) AND ADDRESS(ES)

Health Research, Inc.
Health Research-Roswell Park
Cancer Inst
Elm and Carlton St
Buffalo NY 14263-0001

8. PERFORMING ORGANIZATION

9. SPONSORING / MONITORING AGENCY NAME(S) AND ADDRESS(ES)

U.S. Army Medical Research and Development Command
Fort Detrick, Maryland 21702-5012

10. SPONSOR/MONITOR'S ACRONYM(S)

11. SPONSOR/MONITOR'S REPORT NUMBER(S)

12. DISTRIBUTION / AVAILABILITY STATEMENT

Approved for Public Release; Distribution Unlimited

13. SUPPLEMENTARY NOTES

14. ABSTRACT

Recently, we found that in a PTEN-deficient mouse PCa model, castration induces an immunosuppressive state within the tumor that is concurrent with tumor recurrence. Mechanistically, this response to ADT is mediated by soluble mediators (TNF and CCL2), facilitating communication between tumor, stromal and immune cell populations within the tumor microenvironment. Based on these preliminary data, we hypothesize: Blocking myeloid suppression prevents progression to castration resistant prostate cancer. We test this hypothesis in three aims. Aim 1 examines the mechanism of paracrine TNF signaling between tumor, stromal and myeloid cell populations within the TME, in inducing immune suppression following ADT. Aim 2 tests whether blocking the transit and/or function of myeloid suppressive cell populations prevents CRPC (tumor recurrence following ADT). We also determine the role of PTEN in ADT-induced immune evasion. Aim 3 tests the hypothesis that ADT, in men with locally advanced PrCa, increases serum TNF and CCL2, as well as circulating myeloid cells, by assessing samples from an ongoing clinical study.

15. SUBJECT TERMS

androgen, castration, immunotherapy, prostate, cancer, TNF, CCL2, tumor associated macrophages, CD8 T-cells

16. SECURITY CLASSIFICATION OF:			17. LIMITATION OF ABSTRACT	18. NUMBER OF PAGES	19a. NAME OF RESPONSIBLE PERSON USAMRDC
a. REPORT	b. ABSTRACT	c. THIS PAGE			19b. TELEPHONE NUMBER *(include area code)*
U	U	U	UU	20	

TABLE OF CONTENTS

1. INTRODUCTION:

Most prostate cancer (PCa) deaths are due to castration resistant PCa (CRPC). While androgen deprivation therapy is the standard of care for patients with advanced PCa, nearly universal progression to CRPC occurs 2-3 years after ADT is initiated. Although there have been key advances in the treatment of CRPC, even the best therapies are not curative. One approach to this problem is to improve the initial treatment of advanced prostate cancers, by combining complementary therapies with ADT, to prevent progression of such advanced cancers to CRPC. Immunotherapy, typically employing T-cell 'checkpoint' inhibitors, has provided very durable remissions, verging on cure for a variety of cancer types. However, CPIs have *not* been effective in prostate cancers, perhaps because such cancers are 'cold' (lacking cytolytic CD8 T-cells). Cold tumors may be caused by infiltration of myeloid cell populations – tumor associated macrophages (TAMs) and myeloid-derived suppressor cells (MDSCs) – into the tumor immune cell microenvironment (TIME). In preliminary data accompanying this proposal, we demonstrate that castration of a PTEN-deficient mouse PCa model induces an immunosuppressive state within the tumor that is concurrent with the onset of tumor recurrence. The response to castration/ADT is tri-phasic: a pro-apoptotic regression phase where tumor shrinks, followed by selection for a residual population of resistant stem-like tumor cells and finally recurrent growth as CRPC. Using PCa cell lines to model the first two phases of the response to ADT, we have shown that ADT induces apoptosis, thereby enriching for an ADT-resistant stem/progenitor population that we demonstrate is an *in vitro* source of enhanced TNF production. Mechanistically, in our model system the response to ADT is driven by the soluble mediators TNF and CCL2, which facilitate communication within the TIME. Specifically, a TNF-CCL2-CCR2 paracrine loop is induced between prostate cancer cells and non-tumor cells in the microenvironment: TNF produced by tumor cells acts on myofibroblasts and TAMs to induce CCL2 production, which in turn recruits tumor-associated macrophages (TAMs) and possibly MDSCs. Analysis of public PCa data sets shows TNF and stem/progenitor marker expression are both increased in CRPC, consistent with our hypothesis that ADT drives the development of an immuno-suppressive state via a cytokine switching mechanism that triggers the TNF-CCL2-CCR2 axis in the TIME.

2. KEYWORDS:

androgen, castration, immunotherapy, prostate, cancer, TNF, CCL2, tumor associated macrophages, CD8 T-cells, myeloid-derived suppressor cells, CCR2, TNF receptors, tumor microenvironment

3. ACCOMPLISHMENTS:

What were the major goals of the project?

We proposed that TNF promotes an immunosuppressive state via CCL2, to drive castration-resistant tumor growth.

- Aim 1 determines the role of tumor-microenvironment-derived TNF as a trigger to induce vascular regression following ADT.

- Aim 2 tests our immune suppression hypothesis in three sub-aims.

- Aim 3 tests the hypothesis that ADT administered to men with locally advanced PCa increases serum TNF and CCL2

What was accomplished under these goals?

Accomplished under Aim 1:

We published the results of Aim 1 (determination of the immediate effects of ADT on the tumor vasculature).

Accomplished under Aim 2

We completed the proposed tasks.

Major Task 1: Determine if therapies directed against TNF and/or CCL2 signaling will prevent castrate resistant recurrence. This provides information on whether or not these soluble mediators are acting in as part of a signaling cascade and complements the insight from Aim 1.

Major Task 2: Determine whether therapies in sub-aim 1 inhibit immune suppression. This key sub-aim determines if immune suppression is the driving force behind recurrence.

Major Task 3: assess hi-MYC model. The purpose is to determine if castration induced immune suppression enhances recurrence in a second model of prostate cancer.

In the prior period, we accomplished the goals of Major Task1. The results were detailed in the Year 3 report, and a manuscript is being prepared for submission.

In the prior period, we determined that TNF-CCL2 signaling effects the tumor immune microenvironment, and that both TNFRII-Fc and CCR2 antagonist block the castration-induced immunosuppressive phenotype.

We have subsequently extended characterization of the immunosuppressive tumor immune microenvironment in two mouse models of prostate cancer. We discovered that each model has distinctive immunosuppressive cell populations, but each have increased levels of exhausted CD8 T-cells. Further, each display evidence of dysregulated checkpoint pathway activation that may be targetable therapeutically. The results are detailed below.

A single-cell transcriptome atlas of the non-malignant and malignant prostate

First, we performed deep single cell RNA-sequencing (scRNA-seq) on cells isolated from tumors of two prostate cancer mouse models and normal prostates of their corresponding normal animals (Figure 1A). 29,323 single cells derived from two 16-week-old normal littermate control ($PTEN^{+/+}$, LM) mice and four age-matched Pb-cre4 x $PTEN^{fl/fl}$ (PTEN.KO) mice with prostate cancer were applied for further analysis (Figure 1B). Based on the t-SNE plots, cells were clustered into nine clusters by differentiated expressed genes (DEG) analysis. According to the cell markers from previous studies, these clusters were revealed as: B cells (yellow, marked by Cd79a, Cd79b), Epithelial (blue, marked by Krt8, Krt18), Myeloid I, Myeloid II (green, marked by Lyz2), NK & T cells (orchid, marked by Nkg7, Cd3d, Cd3g, Trbc2), Str.Endothelial.1, Str.Endothelial.2 (purple and navy, marked by Cdh5), Str.Fibroblast (marked by Dcn, Col1a2, Col3a1), and seminal vesicles (SV, marked by Svs2, Svs4 and Svs5).
A total of 16,481 single cells from two 9-month-old FVB normal prostate and two age-matched ARR2Pb-Myc (HiMYC) prostate cancer mouse model passed the quality control (Figure 1C). Similarly, nine distinct clusters were finally identified, including B cells 1, B cells 2, Epithelial, Myeloid, NK & T cells, Str.Endothelial, Str.Fibroblast, SV1 and SV2 based on cluster-specific marker genes identified by DEG analysis. All SV clusters were removed before downstream analyses. Interestingly, the proportion of stromal cells decreased with tumor progression in both mouse models, among which fibroblasts majorly contributed to the reduction (Figure 1D).

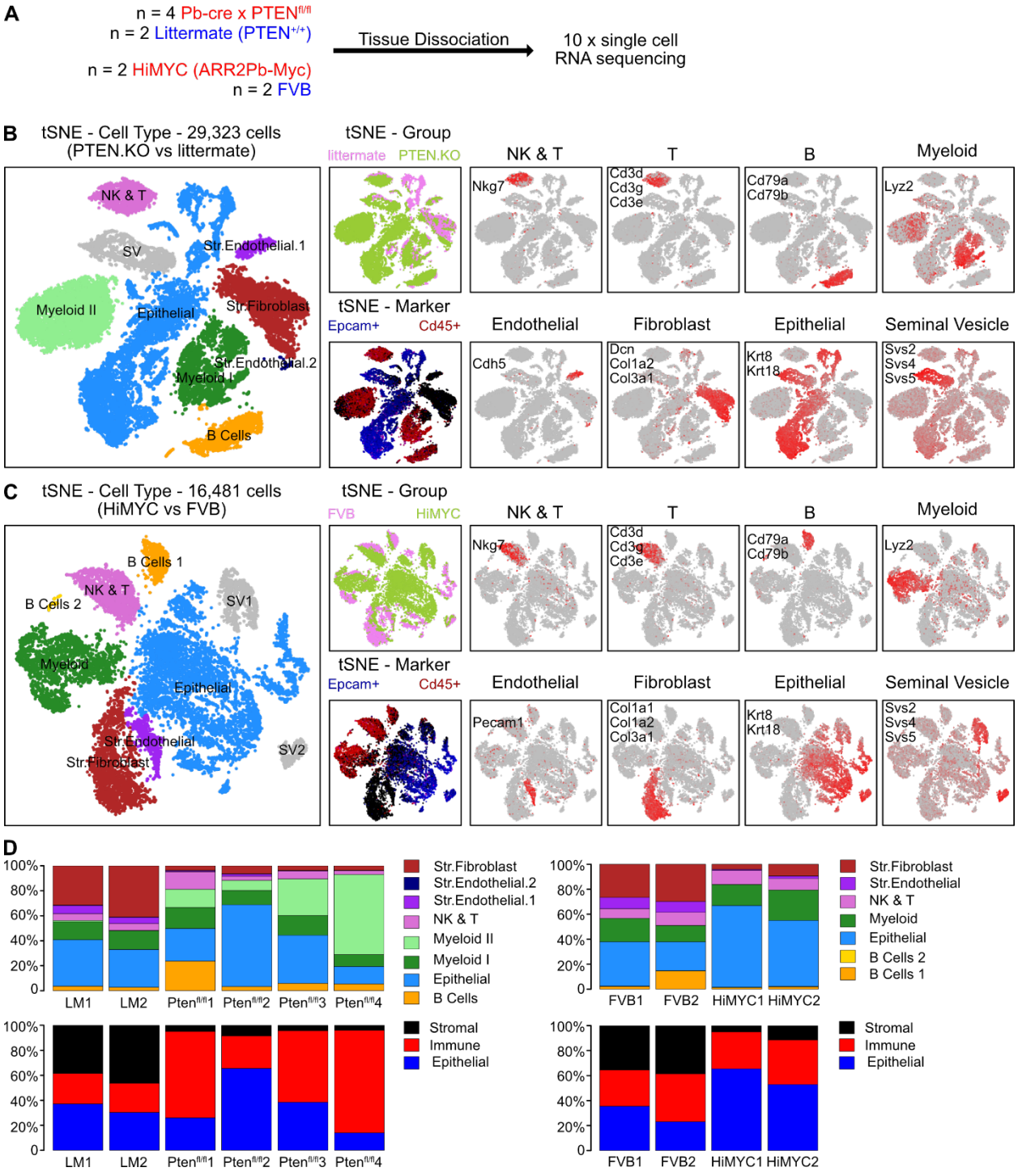

Figure 1. Overview of single cells from two prostate cancer mouse models and corresponding normal prostates.

A. Pipeline of this study. **B.** t-SNE plot of 29,323 single cells from age-matched normal littermate control (PTEN$^{+/+}$) mice (n=2) and Pb-cre4 x PTEN$^{fl/fl}$ mice (n=4) with prostate cancer. Shown is t-SNE plot of the integrated scRNA-seq profiles of from 6 animals but colored by: nine cell subtypes, sample type of origin (PTEN-deficient in yellowgreen or littermate in violet), immune (Cd45, red) /

epithelial (Epcam, blue) markers, and by representative cell type markers. **C.** t-SNE plot of 16,481 single cells from age-matched normal FVB mice (n=2) and ARR2Pb-Myc (Hi-MYC) mice (n=2) with prostate cancer. Shown is t-SNE plot of the integrated scRNA-seq profiles of cells from 4 animals but colored by: nine cell subtypes, sample type of origin (HiMYC in yellowgreen or FVB in violet), immune (Cd45, red) / epithelial (Epcam, blue) markers, and by representative cell type markers. **D.** The fraction of cells from each subtype of each animal.

The immunosuppressive composition of myeloid subtypes in tumor

One distinct 'Myeloid II' cluster was mostly observed in PTEN.KO mice. To uncover the spectrum of myeloid heterogeneity and states, we first utilized t-SNE to re-cluster myeloid cells. Four monocyte/macrophage subsets, Macrophage, Mono.Ace, Mono.Ccr2 and Mono.S100a8 cells, characterized by high expression of Cd14 and low expression of Cd24a, were identified and further distinguished by specific expression of C1qa/C1qb/C1qc, angiotensin-converting enzyme (Ace), Ccr2, and S100a8/S100a9, respectively (Figure 2A-B). Notably, in PTEN.KO and LM, the 'Myeloid II' cluster from Figure 12B expressed high levels of S100a8 and S100a9 and was defined as Mono.S100a8. The Mono.S100a8 cluster served as a major myeloid sub-population in PTEN.KO (Figure 2C). S100A8 has been reported as one of the top 25 upregulated proteins in PTEN.KO mouse prostate (152). The immunosuppressive patterns from PTEN-deficient myeloid cells were mainly from the unique Mono.S100a8 cluster. Compared with the FVB mice, the Mono.Ccr2 proportion increased in HiMYC myeloid cells (Figure 2D).

The remaining clusters were identified as dendritic cells (DC). The immature DC expressed lower levels of costimulatory molecules, including Cd80, Cd83, Cd86, and MHC II (H2-Aa and H2-Ab1) (Figure 2E-F). The Cd103.DC expressed high level of Itgae (Cd103), together with other conventional DC1 (cDC1) markers, such as Xcr1, Btla and transcription factors Irf8 and Batf3 (153). cDC1 are critical for eliciting anti-tumor T cell responses. The proportions of Cd103.DC in PTEN.KO and HiMYC myeloid cells decreased. The Cd11b.DC were distinguished by Itgam (Cd11b), governed by the conventional DC2 (cDC2) marker transcription factor Irf4. Batf3 expression was also detected in Cd11b.DC. Batf3 is expressed in both Ifr8-positive and Ifr4-positive cDC, however, Batf3 is developmentally required only for Irf8+ cDC (154). Cd209.DC were $Cd103^{-}Cd11b^{+}$ cells with high Cd209a, Clec10a (Cd301) and Klrd1 expression. The mig.DC (migratory DC) were defined by Ccr7, which is necessary to direct DC to lymph nodes and to elicit an adaptative immune response (155). The Mo.DC (monocyte-derived DC) highly expressed Mrc1 were only found in PTEN.KO and LM.

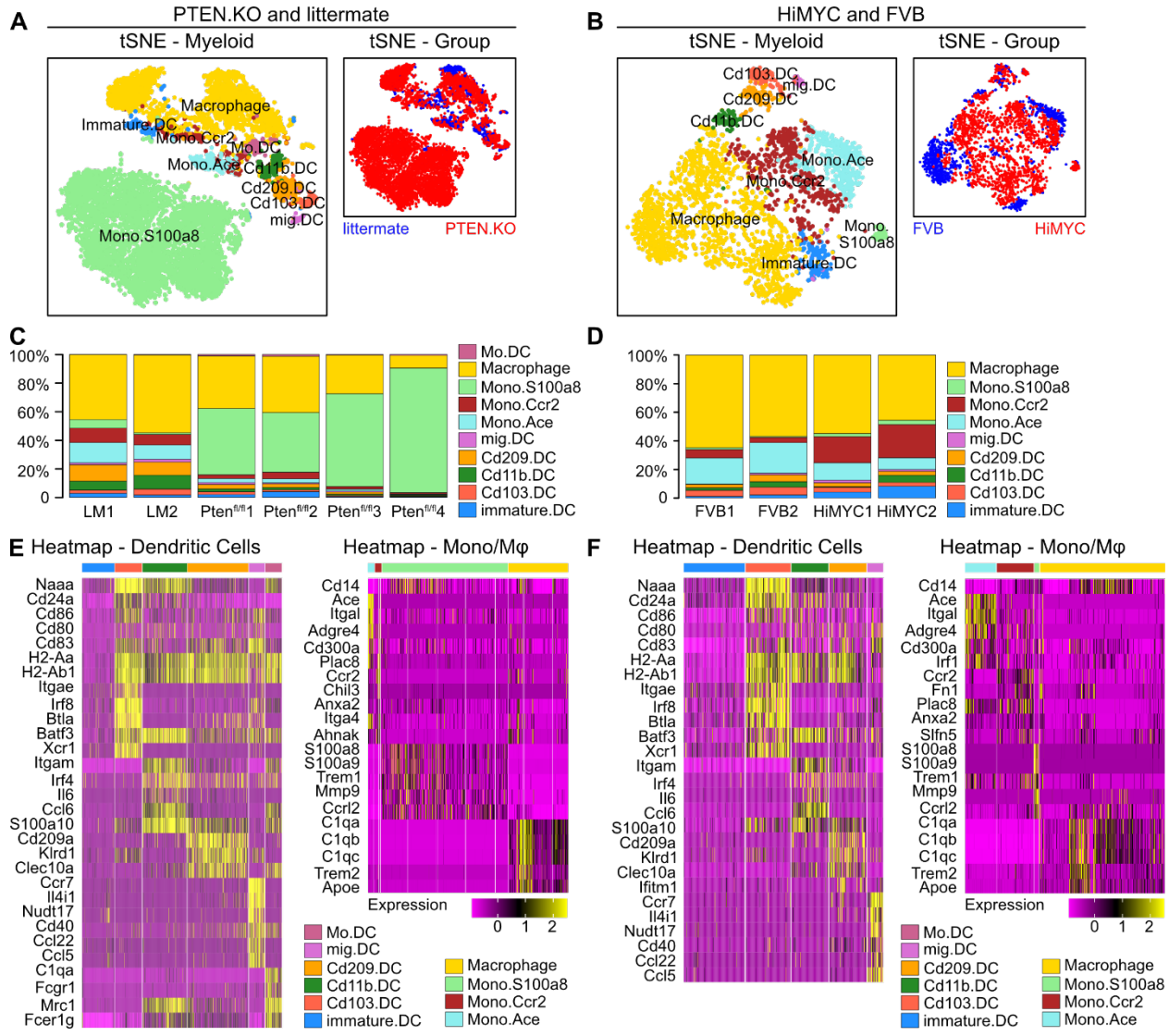

Figure 22. Diversity within the myeloid cell lineage and functionality of cancer vs normal. **A.** tSNE visualization of myeloid cell subtypes (left) and group (right) in PTEN.KO (red, n=4) and LM (blue, n=2). **B.** tSNE visualization of myeloid cell subtypes (left) and group (right) in HiMYC (red, n=2) and FVB (blue, n=2). **C.** Composition of myeloid subtypes for PTEN.KO and LM. **D.** Composition of myeloid subtypes for HiMYC and FVB (right). **E.** Heatmap of selected markers and functional genes in PTEN.KO and LM dendritic cells (left) and monocytes/macrophages (right). **F.** Heatmap of selected markers and functional genes in HiMYC and FVB dendritic cells (left) and monocytes/macrophages (right).

Detailed analysis of NK/T cells uncovered T cell dysfunction in prostate cancer

We then subset and analyzed the NK/T cluster. Within PTEN.KO and LM NK/T cells, we identified CD4+ naïve T cells (CD4.T_N), CD4+ exhausted T cells (CD4.T_{EX}), CD4+ Tregs (CD4.T_{REG}), CD4+ T helper 17-like T cells (CD4.Th17), CD8+ naïve T cells (CD8.T_N), CD8+ exhausted T cells (CD8.T_{EX}), CD8+ effector T cells (CD8.T_{EFF}), tissue resident memory T cells (T_{RM}), and Natural Killer (NK) cells according to expression of their respective markers (Figure 3A-B). Within Hi-MYC and FVB NK & T cells, re-clustering revealed 7 clusters: naïve T cells (T_N), CD4.T_{REG}, CD4.Th17, CD8.T_{EX}, CD8.T_{EFF}, T_{RM}, and NK cells according to expression of their respective markers as shown in the heatmap (Figure 3C-D).

Naïve T cells expressed high level of Ccr7 together with naïve markers including Lef1, Tcf7 and Sell (Cd62l). CD8+ T cells were determined by Cd8a and Cd8b1, while CD4+ T cells were separated by Cd4 and Il7r. CD8.T_{EX} was defined based on by low Ccr7 expression and high expression of pre-dysfunctional marker granzyme K (Gzmk) and dysfunctional markers (Pdcd1, Ctla4 and Lag3) (156). CD8.T_{EFF} showed low Ccr7 and low expression of exhaustion markers with expression of cytotoxicity related Ifng, Ccl4, Ccl5 and Gzma. CD4.T_{REG} expressed high Il2ra (Cd25), Foxp3 and Ctla4. CD4.Th17 were separated based on Rorc and overexpression of Tmem176a/b (157,158). T_{RM} were characterized by Itgae (Cd103). The distributions of the identified T cells subsets are shown in Figure 3E. Relative to normal prostate controls, we observed a higher proportion of CD8.T_{EX} and immunosuppressive CD4.T_{REG} cells in both PTEN.KO and Hi-MYC tumors.

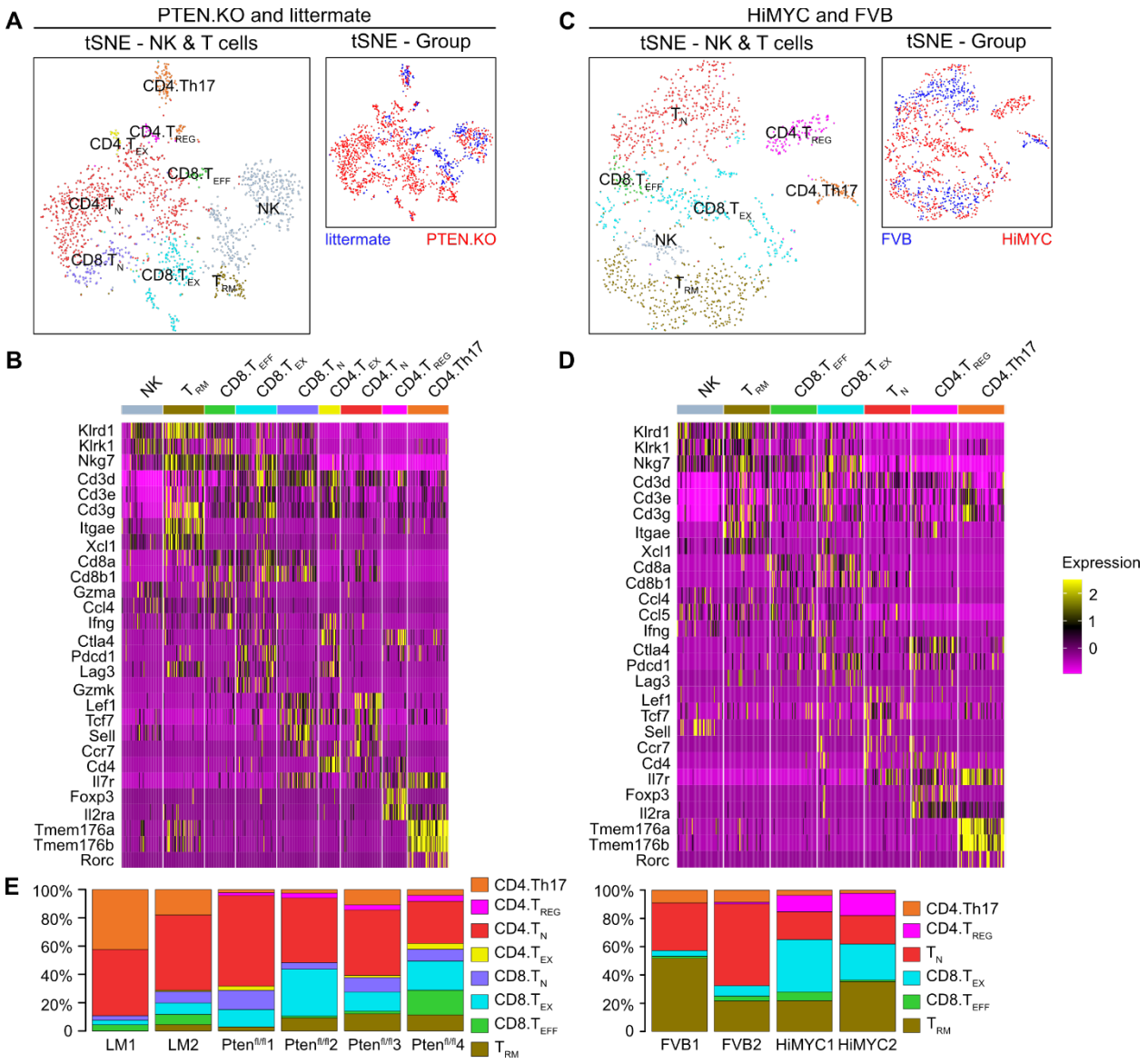

Figure 3. Diversity within NK/T cells of cancer vs normal

A. tSNE visualization of NK cell and eight T cell subtypes (left) and group (right) in PTEN.KO (red, n=4) and LM (blue, n=2). **B.** Heatmap of selected markers and functional genes in PTEN.KO and LM NK and T cells. **C.** tSNE visualization of NK cell and six T cell subtypes (left) and group (right) in HiMYC (red, n=2) and FVB (blue, n=2). **D.** Heatmap of selected markers and functional genes in HiMYC and FVB NK and T cells. **E.** Composition of T cell subtypes for PTEN.KO and LM (left) and HiMYC and FVB (right).

To validate our findings, we next applied pseudotime analysis to reconstruct developmental trajectories in CD4$^+$ T cells. The pseudotime analysis revealed different gradient of CD4$^+$ T cell differentiation in both models (Figure 4). Both progressions to CD4.T$_{REG}$ started with naïve T cells. In PTEN.KO, a subset of persisting T$_N$ cells directly differentiated into CD4.T$_{REG}$. However, HiMYC CD4.T$_{REG}$ were started with T$_N$ and then CD4.Th17. Another branch of T$_N$ cells progressed along the naive-memory differentiation axis to T$_{RM}$.

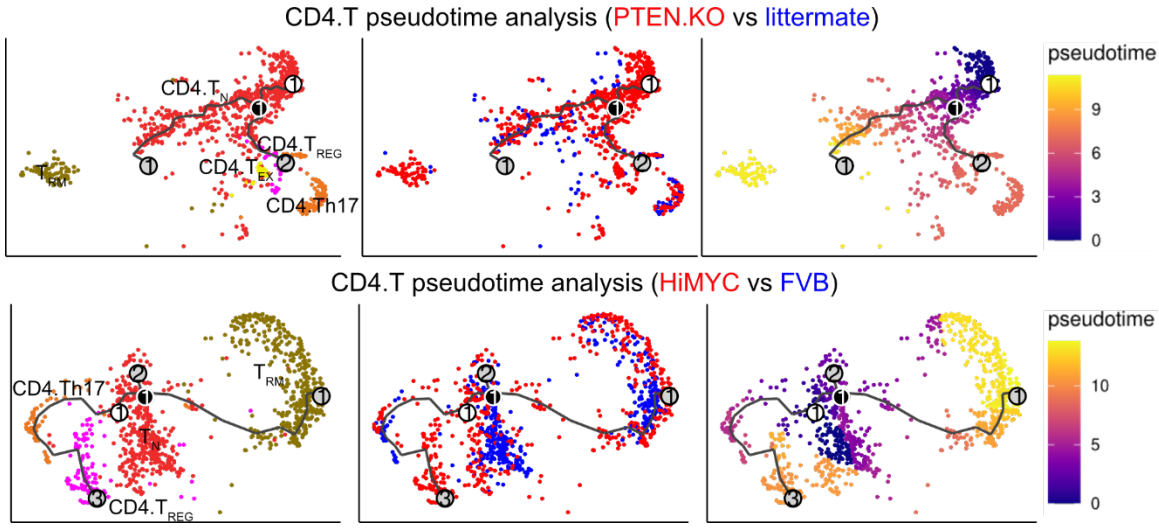

Figure 4. Pseudotime analysis reveals distinct trajectories of CD4+ T cell differentiation. Branched pseudotime trajectory (from Monocle3), each cell is colored by its subtype label (left panel; naïve T cells in red, Th17 in orange, T$_{REG}$ in purple, exhausted CD4 cells in yellow, and T$_{RM}$ in brown), its group (middle panel; tumor models in red and normal prostates in blue), or pseudotime value (right panel; pseudotime colored according to the bar).

Attenuated CD226-Nectin2 interaction in tumor

To explore and compare potential interactions between cell types identified in our datasets, we performed CellChat (149) analysis on both murine normal prostate and prostate tumor (Figure 5A-B). By comparing the overall communication probability between murine normal prostate and prostate tumor, we found that 7 signaling pathways (ANGPTL, BMP, CD226, NOTCH, OCLN, PTN, and SEMA7) were highly active in both LM and FVB. Relative to their corresponding controls, 6 signaling pathways (ALCAM, CD6, CDH1 COMPLEMENT, MPZ, and OSM) were stronger in both PTEN-deficient and Hi-MYC mice (Figure 5C).

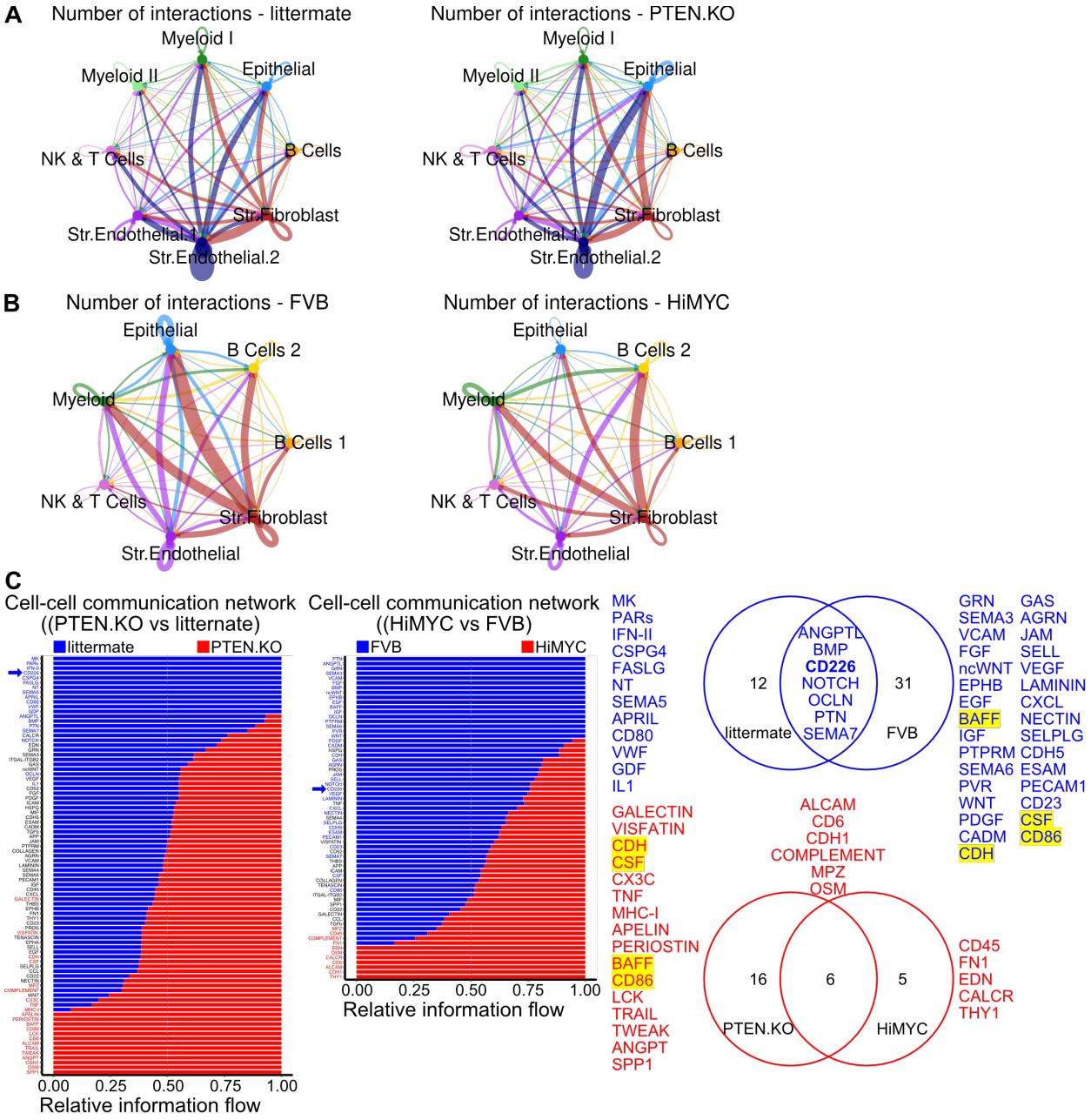

Figure 4. Crosstalk between epithelial cells and microenvironment.
A. Circle plots showing the number of interactions of epithelial cells, immune cells and stromal cells in LM (left, n=2) and PTEN.KO (right, n=4). The line thickness is proportional to the number of ligands when cognate receptors are present in the recipient cell type. The loops indicate autocrine circuits. **B.** Circle plots showing the number of interactions of epithelial cells, immune cells and stromal cells in FVB (left, n=2) and HiMYC (right, n=2). **C.** All significant signaling pathways were ranked based on their differences in overall information flow within the inferred networks between prostate tumors and normal prostates. The top signaling pathways colored blue are more enriched in normal prostates, the middle ones colored black are equally enriched in tumor and normal prostate, and the bottom ones colored red are more enriched in two transgenic mouse models.

We then identified ligand-receptor pairs from immune cells targeting epithelial cells that are significantly enriched (Figure 6). Table depicts imputed pathway activity for the indicated cell pairs, and dot color reflects communication probabilities while dot size represents computed p-values. Specifically, we discover that the ligand-receptor pair CD226-Nectin2 was one shared significant signaling by normal prostates, contributing to the communication from 'NK & T' to 'Epithelial'.

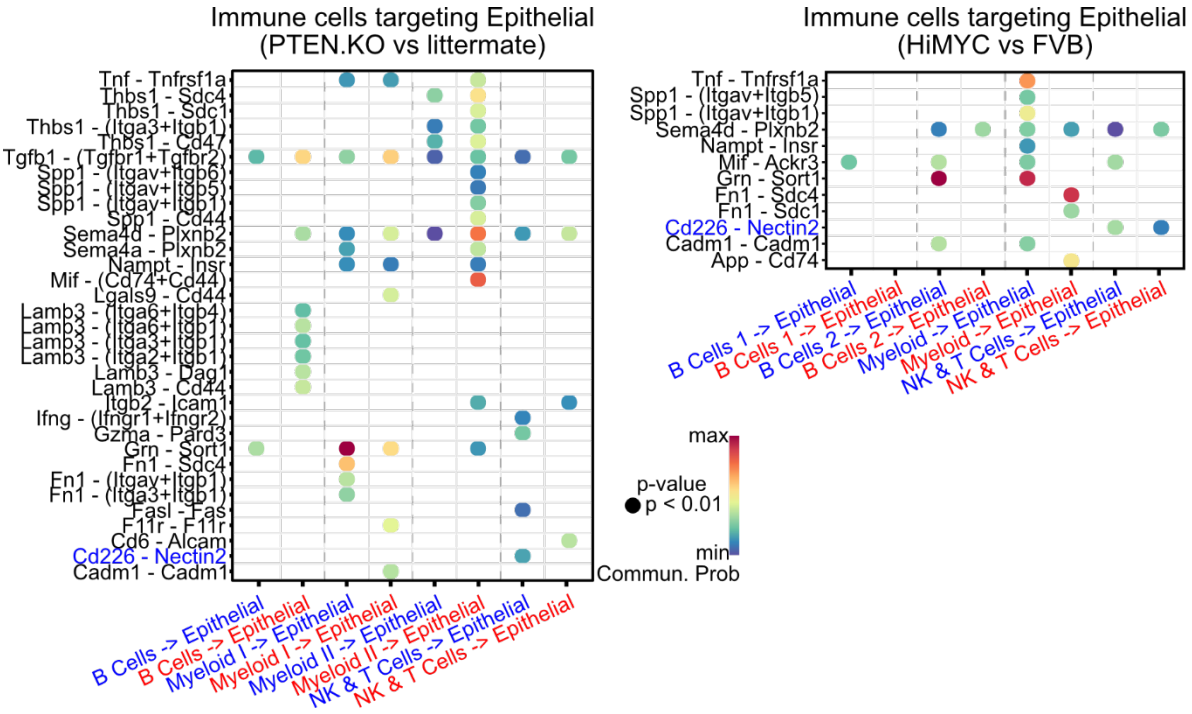

Figure 65. Summary of ligand-receptor interaction from immune cell targeting epithelial cells. Ligand-receptor interactions from normal prostates (littermate or FVB) are shown at the bottom in blue, while ligand-receptor interactions from tumors (PTEN.KO or HiMYC) are shown in red. Among them, attenuated Cd226-Nectin2 in tumor infiltrating NK/T towards epithelial cells was observed (highlighted in blue).

CD226 was downregulated in prostate cancer lymphocytes

Since attenuated CD226-Nectin2 interaction was observed in both tumor mouse models, we first examined the role of CD226 expression in NK and T cells. A large proportion of NK and T cells were Cd226-negative (Cd226.neg). Lower percentage of Cd226-positive cells (Cd226.pos) indicates CD226 deficiency in tumor NK and T cells in both PTEN-deficient and Hi-MYC mice (Figure 7A). We then divided NK and T cells into CD8.T, CD4.T and NK based on their expression of CD8/CD4/NK related genes. The proportion of the Cd226.pos population within the CD8.T cells, CD4.T cells and NK cells all decreased in tumor (Figure 7B).

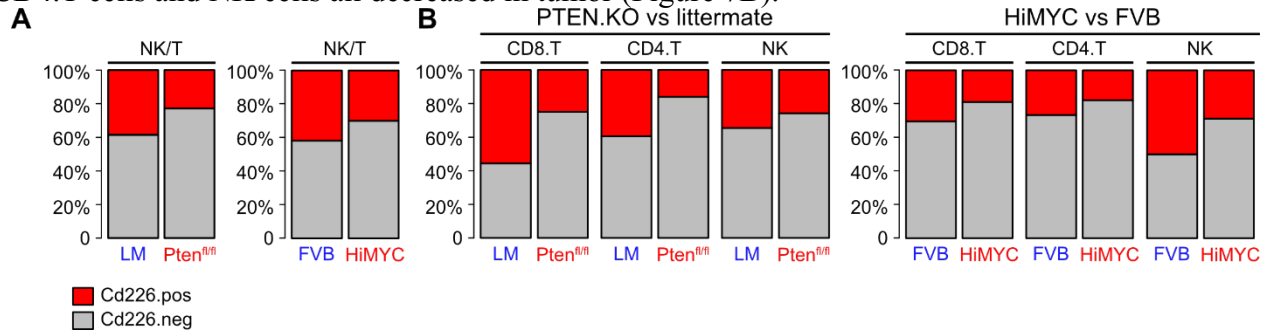

Figure 7. Proportion of Cd226-positive NK and T cells.
A. Barplots showing the percentages of Cd226-positive (Cd226.pos, red) and Cd226-negative (Cd226.pos, gray) NK and T cells in littermate compared with PTEN-deficient mice (left) and FVB together with HiMYC (right). **B.** Barplots showing the percentages of Cd226-positive (Cd226.pos, red) and Cd226-negative (Cd226.pos, gray) CD8 T cells, CD4 T cells and NK cells in littermate compared with PTEN-deficient mice (left) and FVB together with HiMYC (right).

Given that CD226 is an activating receptor on NK and T cells, we hypothesized that CD226 mRNA expression correlated with genes involved in activation/effector function. Cd226.pos NK and T cells were associated with higher expression of cytotoxic lymphocyte functional genes including Ifng, Gzmb and Xcl1 whether derived from normal prostate or prostate tumor (Figure 8A). Cd226.neg CD8.T cells appeared to be dysfunctional with reduced expression of Ifng, Gzmb and Xcl1 (Figure 8B).

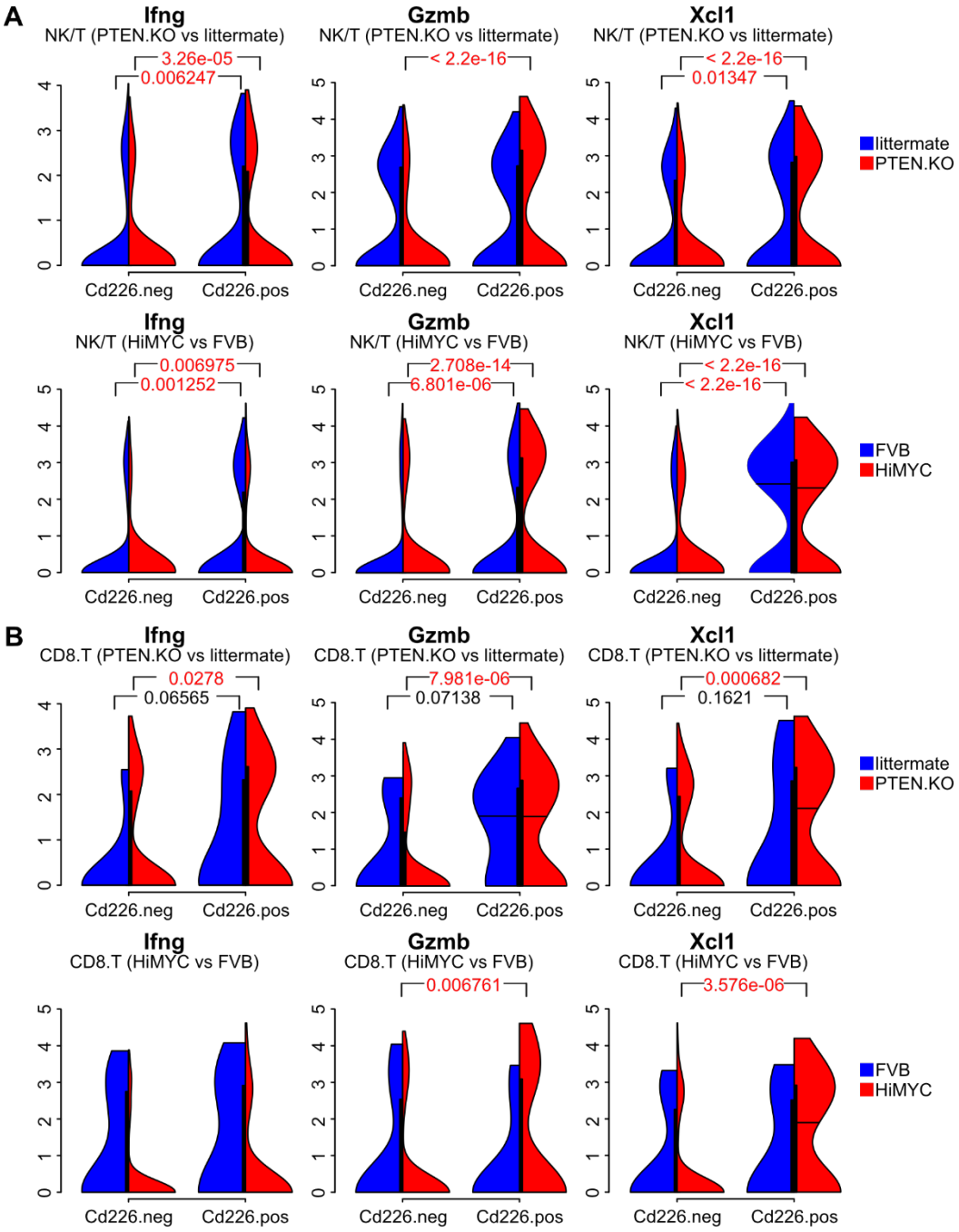

Figure 8. Cd226 expression correlates with effector function genes in prostate NK and T cells. **A.** Relative expression of Ifng, Gzmb and Xcl1 in NK and T cells across Cd226 subsets. **B.** Relative expression of Ifng, Gzmb and Xcl1 in CD8 T cells across Cd226 subsets. Cells from littermate or FVB are shown in blue, while cells from PTEN-deficient or HiMYC are shown in red. A t-test was used to compare the expression difference between tumor and normal tissue. Values are mean ± SEM. TPM, transcript per million.

We further examined Cd226 expression levels on the 'NK & T cells' cluster (Figure 9A). Cd226 was significantly downregulated in PTEN-deficient as well as Hi-MYC NK/T cells. Interaction between CD226 and CD155 (PVR) or CD112 (Nectin-2) enhances T cell activation, while TIGIT competes for binding the same ligands and thus inhibits T cell responses (135) (Figure 9B). Tigit expression levels increased on Tigit-positive NK and T cells in both tumor models (Figure 9C).

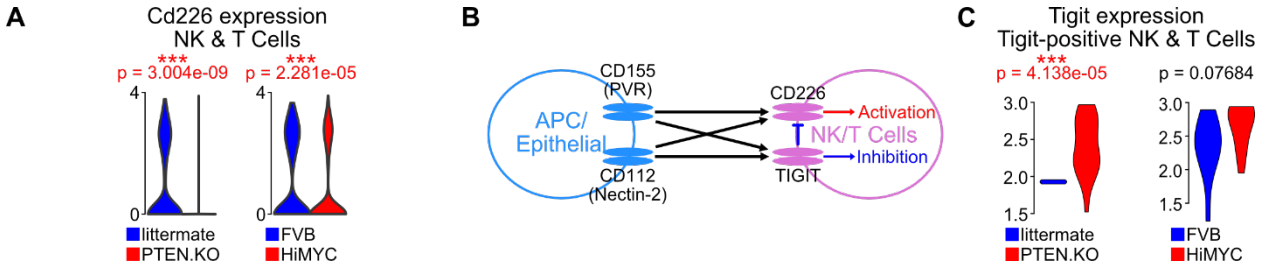

Figure 9. Cd226 and Tigit expression in NK and T cells.
A. Violin plots showing decreased Cd226 mRNA expression from NK and T cells. NK and T cells from littermate or FVB are shown in blue and NK and T cells from PTEN-deficient or HiMYC are shown in red. **B.** CD226 and TIGIT model in immune response. Both CD226 and TIGIT are primarily expressed on NK or T cells (purple) and interact with PVR or Nectin-2 expressed on epithelial cells or antigen-presenting cells (APC, blue). CD226-PVR or CD226-Nectin2 deliver an immune activation signal, while TIGIT-PVR or TIGIT-Nectin2 transmits inhibitory signals. **C.** Tigit expression on Tigit-positive NK and T cells increased in tumors (red).

Accomplished under Aim 3

In Aim 3, we continue to collect and store samples for future batch-wise analysis. We have enrolled 4 participants in Arm A (ADT only, target 10) and accrued biospecimens from 2 of these (the therapy paradigm has evolved precluding additional participants in accord with standard of care therapy, and this Arm will close upon completion of the study not fully enrolled). We have enrolled 25 participants in Arm B (ADT plus EBRT, target 20) and accrued biospecimens from 23 of these (we are closing this Arm in September 2023). We have enrolled 11 participants in Arm C (EBRT only, target 20) and accrued biospecimens from 9 of these. As with Arm A, fewer prostate cancer patients are electing EBRT only, and so accrual to this arm has become more difficult during the course of this study. Upon completion of biospecimen accrual, analysis will commence.

What opportunities for training and professional development has the project provided?
Dr. Zhang received her Ph.D. degree based on her work on this project.

How were the results disseminated to communities of interest?
Nothing to report.

What do you plan to do during the next reporting period to accomplish the goals?

We will prepare a manuscript documenting our results from Aims 2. We intend to test our immunosuppressive findings as targets in preclinical models. We plan on competing enrollment for the study of Aim 3, and undertake biospecimen analysis for TNF and CCL2.

4. IMPACT:

What was the impact on the development of the principal disciplines of the project?

We previously demonstrated that demonstrated that castration led to tumor regression in a PTEN-deficient mouse model, followed by the expansion of a basal stem-like cell population and TNF secretion, likely from this basal stem-like population. At the late (~5 week) time point, increased TNF secretion correlated with tumor recurrence and TNF-induced, NFkB-mediated CCL2 secretion. CCL2 production, in turn, recruits TAMs, reduces CTLs and enhances tumor proliferation and recurrence. Indeed, CD68-stained cells (presumptive TAMs) increased and CD8 T cells (presumptive cytolytic T-lymphocytes; CTLs) decreased after castration, just as tumor re-growth in the recurrence phase is beginning. Etanercept and CCR2 antagonist partially blocks these changes and coordinately inhibits tumor recurrence. Single-cell transcriptomic analysis determined that CD8 / CD68 ratio predicts castration outcome and suggests that immune suppression drives tumor re-growth. We employed single-cell RNA sequencing (scRNAseq) to characterize the normal and neoplastic immune landscape in murine models of prostate cancer. Specifically, we profiled the transcriptomes of 45,804 single cells from 10 mice spanning two genetically engineered mouse models and the corresponding normal prostates. One model is driven by prostate-specific PTEN deficiency (PTEN.KO) and the other by prostate-specific MYC-overexpression (Hi-MYC). The tumor microenvironment is marked by a sharp reduction in stromal cells (both fibroblasts and endothelium) relative to the normal prostate. The two models show distinct differences in the populations that replace the stromal cells: a

distinctive S100a8 monocyte population in the PTEN.KO model and an epithelial cell population in the Hi-MYC model. However, both models developed exhausted CD8 T cells and regulatory CD4 T cells, consistent with an immunosuppressive TiME. We used CellChat, an algorithm that quantitatively analyzes intercellular communication networks and – compared with normal prostate – both murine models showed attenuated expression of the T-cell activating receptor CD226, which could lead to lymphocyte dysfunction. This suggests therapies that modulate the CD226/TIGIT axis may show therapeutic efficacy in these preclinical models of prostate cancer.

What was the impact on other disciplines?
Nothing to report

What was the impact on technology transfer?
Nothing to report

What was the impact on society beyond science and technology?
Nothing to report

5. CHANGES/PROBLEMS:

Nothing to report

Changes in approach and reasons for change

Actual or anticipated problems or delays and actions or plans to resolve them

Since Dr. Zhang's graduation, she has not been participating in data analysis and writing manuscripts. The lab is following up on her findings and when sufficient tumor-bearing mice are available, a technician in the lab will test whether neutralizing the new therapeutic target controls tumor growth using the resources/funds remaining. Dr. Nastiuk will continue analysis of the data and drafting manuscripts reporting results from this award enabled investigation.

Changes that had a significant impact on expenditures

Personnel departures continue to result in unanticipated funds remaining at the end of the initial performance period. A second no-cost extension was approved by the grants and program officer to complete the proposed tasks.

Significant changes in use or care of human subjects, vertebrate animals, biohazards, and/or select agents

Nothing to report

6. PRODUCTS:

Publications.

Nothing to report

Other publications, conference papers and presentations.

Nothing to report

Website(s) or other Internet site(s)
Nothing to report

Technologies or techniques
Nothing to report

Inventions, patent applications, and/or licenses
Nothing to report

Other Products
Nothing to report

7. PARTICIPANTS & OTHER COLLABORATING ORGANIZATIONS

What individuals worked on the project?

Kent Nastiuk, PhD. PI, 0.9 Calendar Months

- Dr. Nastiuk lead the project and analysis of the data for manuscript #2.

During the first NCE year, Drs. Maolake, Jaiswal, Eng, Xu, Chatta, and Krolewski were no longer participating in the project. Ms. Zhang and Ms. Herrington are no longer participating in the project.

Has there been a change in the active other support of the PD/PI(s) or senior/key personnel since the last reporting period?

Dr. Nastiuk will end his previous 0.9 Calendar months support from W81XWH-19-0397 for the approved second NCE year of this project. The remaining funds will be used for animals, imaging costs, and supplies to test the immunosuppressive target hypothesis generated in the prior period.

Dr. Nastiuk no longer has his previous 0.9 Calendar months support from W81XWH-19-0397, entitled "Hereditary X-linked Tumor Suppressor Escapes Immune Control in Prostate Cancer" during the NCE year of this project. This project has terminated.

What other organizations were involved as partners?
None

8. SPECIAL REPORTING REQUIREMENTS

Nothing to report

9. APPENDICES:

None